Vibration reduction of structural-acoustic systems using synchronized switch damping techniques

Monica Ciminello, Jean-François Deü, Roger Ohayon, Salvatore Ameduri

VIBRATION REDUCTION OF STRUCTURAL-ACOUSTIC SYSTEMS USING SYNCHRONIZED SWITCH DAMPING TECHNIQUES

Monica Ciminello **Jean-François Deü** **Roger Ohayon**

Conservatoire National des Arts et Métiers (CNAM)
Structural Mechanics and Coupled Systems Laboratory, Chair of Mechanics
2 rue Conté, 75003 Paris, France
email: monicacimm@libero.it ; deu@cnam.fr ; ohayon@cnam.fr

Salvatore Ameduri

Italian Aerospace Research Centre (CIRA)
Smart Structures Laboratory, Via Maiorise, Capua, Italy
email: s.ameduri@cira.it

ABSTRACT

In this paper we present numerical results concerning vibration reduction of structural-acoustic systems using the synchronized switch control technique. In order to develop a general procedure to model the coupled system (composed by the fluid domain, the structure and the piezoelectric elements), the idea is to use the performances of a standard commercial code such as Nastran. A symmetric reduced order model is derived from a general finite element description through the extraction of appropriate system matrices. For sake of brevity, we just recall that depending upon the choice of fluid field variables, non symmetric formulations are usually obtained (so-called displacement-pressure formulations), the symmetrization can be derived through appropriate choice of fluid field variables [1,2]. A simple fluid-structure system for which an analytic solution exists will be used to verify the finite element results and to demonstrate the capabilities of the control procedure. Referring to experimental tests [3], the system consists of a straight air-filled tube with a square cross section. The tube is a rigid cavity with an elastic plate at one end and a piezoelectric patch bonded in its centre. Firstly, the conservative structural-acoustic problem is presented. The symmetric variational and finite element formulations are then described. The model is constructed using Nastran software and the finite element matrices are then extracted and assembled in Matlab. In a second step, the electro-mechanical coupling matrices are built using three-dimensional finite elements in order to take into account local moments of the piezoelectric wafers according to the equivalent thermal coefficient theory [4,5]. Finally, the reduced electro-mechanical fluid-structure system, obtained through a modal projection, is integrated in time using a Newmark type algorithm. Numerical results are then presented showing the performance of the synchronized switch damping for vibro-acoustic applications in the low frequency domain (low modal density).

INTRODUCTION

In acoustic wave control field, as well as in the vibration control field, the trend is to use active technique that seems to be one of the most efficient strategies to reduce the noise level, at a wide broadband range, despite a complexity of the design and an external power supply required. Actually, for the purpose of noise reduction, the approach is to reduce acoustic radiation field through the vibration reduction of the structure, since the structure itself may be a noise source. A considerable amount of works deals with the numerical or experimental development of techniques of noise reduction using piezoelectric devices bonded or embedded in structural elements.

Kim and Ko [6] worked on finite element modeling for piezoelectric structures. The optimization procedure shows the best location of the actuators and sensors are close to those regions where the strain is maximal. The active control system implemented is a negative feedback. To take into account the acoustic pressure in the cavity the modal approach is used invoking the orthogonality of the modes shapes. The principal

advantage of this approach is the reduction of the size of the system equation.

Another approach is to combine active and passive devices. Ro and Baz [7] presented a work in which the sound radiation from a vibrating flat plate coupled with an acoustic cavity is controlled. The sound radiation is controlled using a single patch of active constrained layer damping. Dynamic and acoustic finite element model are developed to study the fundamental phenomena governing the coupling between the dynamics. The models are used to compute the frequencies, mode shapes and sound radiation for different control gains. The experimental results obtained indicate amplitude attenuation of 27, 54, and 75% with respect to uncontrolled plate, for controlling gains of 62, 250, 500 respectively for the first resonance frequency.

A different approach for noise reduction of sound radiating into a cavity is presented by Guyomar [8]. The work deals with the semi passive approach in which the synchronized switch damping technique is implemented and the piezoelements are continuously switched from the open circuit state to a specific electric network synchronously with the strain. The authors describe the experimental results consisting in exciting the plate via the loudspeaker and detect the noise level of the sound wave transmitted in the external environment. The plate vibrations speed is monitored in the center of the plate which corresponds to a maximum deflection for each mode. The measure is made and compared in three cases: without control, with an inductive switched shunt and with a voltage driving inductive switched shunt. A microphone monitors the pressure of the acoustic wave transmitted through the plate at different locations. A maximum attenuation of 15 dB on the transmitted wave pressure is obtained.

In the present paper we present a finite element modeling to simulate noise and vibration reduction of acoustic cavity through piezo in switched shunt configuration. In the first section we establish the variational formulation of the fluid structure coupled problem and the corresponding matrix equations. The aim is to establish a variational formulation in view of a direct treatment by finite elements. In the second section we assemble the fluid structure equation with the electro mechanical matrices of piezo device and finally the electrical contributions of the shunt circuit. The third section is dedicated to the numerical integration of the reduced model of the full coupled system. Due to the switching mechanism and the quick commutation time, the system is not linear, so a direct transient response in time domain will be computed. For this purpose a classical Newmark algorithm will be used.

THE ELASTO-ACOUSTIC PROBLEM

Several finite element formulations have been proposed in literature for modeling elasto-acoustic coupled systems at the fluid structure interface. A symmetric reduced order model is derived from a general finite element description through the extraction of appropriate system matrices. For sake of brevity, we just recall that depending upon the choice of fluid field variables, non symmetric formulation are usually obtained (so-called displacement-pressure formulations) and the symmetrization can be derived through appropriate choice of fluid field variables [1,2]. A symmetric formulation can be obtained, for example, using the fluid velocity potential [1]. It must be noted that the velocity potential formulation has the disadvantage that it leads to a symmetric but artificial damping matrix which makes it necessary to use complex eigenvalue solvers. In what follows we recall the finite element formulation of the fluid structure coupled problem. For more details, the reader is referred to the book of Morand and Ohayon [1].

Local equation of the fluid structure coupled system

Let us present now the local conservative equation of the fluid structure coupled system in time domain in function of the structural displacement u, and the fluid pressure p [1]. Let us consider the vibrations of an elastic structure, occupying the volume Ω_S, interacting with a homogeneous, inviscid and compressible fluid, occupying the volume Ω_F, neglecting gravity effects. The fluid structure interface is noted as Σ. The structure is clamped at one part of the boundary Γ_u and an external excitation t acts on the structural surface Γ_t. The local equations of the problem are given by:

$$\operatorname{div}\sigma(u) = \rho_S \frac{\partial^2 u}{\partial t^2} \quad in \quad \Omega_S \tag{1}$$

$$u = 0 \quad on \quad \Gamma_u \tag{2}$$

$$\sigma(u) n_S = t \quad on \quad \Gamma_t \tag{3}$$

$$\sigma(u) n_S = pn \quad on \quad \Sigma \tag{4}$$

$$\nabla p \cdot n = -\rho_F \frac{\partial^2 u}{\partial t^2} \cdot n \quad on \quad \Sigma \tag{5}$$

$$\nabla p = \frac{1}{c_F^2} \frac{\partial^2 p}{\partial t^2} \quad on \quad \Omega_F \tag{6}$$

with appropriate initial condition.

The first corresponds to the elastodynamics equation in absence of body force; the second is the constrained boundary condition; the third is the external load boundary condition; the fourth is resulting from the action of pressure forces exerted by the fluid on the structure; the fifth is the kinematic interface fluid-structure condition; the sixth corresponds to the Helmholtz equation.

Variational formulation of the fluid structure coupled system

In order to derive the variational formulation we use the test function method. We proceed in two steps, treating successively the equations relating to the structure (subject to fluid pressure actions), then the equations relating to the fluid (subject to a wall displacement).

First, we introduce the space C_u of the regular functions u defined in Ω_S and time independent. Multiplying Equation (1) by any function-test δu of C_u, such that $\delta u=0$ on Γ_u, and then applying the Green's formula and taking into account the boundary conditions (2, 3, 4) we obtain:

$$\int_{\Omega_S} \mathrm{tr}\left[\sigma(u)\varepsilon(\delta u)\right]dv + \int_{\Omega_S} \rho_S \frac{\partial^2 u}{\partial t^2}\cdot\delta u dv - \int_{\Sigma} pn\cdot\delta u ds = \int_{\Gamma_t} t\cdot\delta u ds \qquad (7)$$

In the second step, we consider the space C_p of the regular functions p defined in Ω_F and time independent. Multiplying Equation (6) by any function-test δp of C_p, and then applying the Green's formula taking into account the boundary condition Equation (5), we obtain:

$$\frac{1}{\rho_F}\int_{\Omega_F} \nabla p\cdot\nabla\delta p dv + \frac{1}{\rho_F c_F^2}\int_{\Omega_F}\frac{\partial^2 p}{\partial t^2}\cdot\delta p dv + \int_{\Sigma}\frac{\partial^2 u}{\partial t^2}\cdot n\delta p ds = 0 \qquad (8)$$

Finally the variational formulation of the fluid structure coupled problem consists in finding $(u,p)\in (C_u\times C_p)$ verifying Equations (7) and (8).

Finite element formulation of the fluid structure coupled system

The matrices corresponding to the linear or bilinear forms involved in the variational formulation (7) and (8) are defined by:

$$\begin{aligned}
&\int_{\Omega_S} \mathrm{tr}\left[\sigma(u)\varepsilon(\delta u)\right]dv \Rightarrow \delta U^T K_u U\\
&\int_{\Omega_S} \rho_S \frac{\partial^2 u}{\partial t^2}\cdot\delta u dv \Rightarrow \delta U^T M_u \ddot{U}\\
&\int_{\Sigma} pn\cdot\delta u ds \Rightarrow \delta U^T C_{up} P\\
&\int_{\Gamma_t} t\cdot\delta u ds \Rightarrow \delta U^T F
\end{aligned} \qquad (9)$$

and

$$\begin{aligned}
&\frac{1}{\rho_F}\int_{\Omega_F} \nabla p\cdot\nabla\delta p dv \Rightarrow \delta P^T K_p P\\
&\frac{1}{\rho_F c_F^2}\int_{\Omega_F}\frac{\partial^2 p}{\partial t^2}\cdot\delta p dv \Rightarrow \delta P^T M_p \ddot{P}\\
&\int_{\Sigma}\frac{\partial^2 u}{\partial t^2}\cdot n\delta p ds \Rightarrow \delta P^T C_{up}^T \ddot{U}
\end{aligned} \qquad (10)$$

In the Equations (9) and (10) U and P represents the degrees of freedom vectors for the structural displacement and the fluid pressure, respectively. The matrix system corresponding to (7) and (8) can be written as follows:

$$\begin{bmatrix} M_u & 0\\ C_{up} & M_p\end{bmatrix}\begin{Bmatrix}\ddot{U}\\ \ddot{P}\end{Bmatrix}+\begin{bmatrix} K_u & -C_{up}\\ 0 & K_p\end{bmatrix}\begin{Bmatrix}U\\ P\end{Bmatrix}=\begin{Bmatrix}F\\ 0\end{Bmatrix} \qquad (11)$$

As previously mentioned, a symmetric formulation can be obtained by introducing the velocity potential ψ [1]:

$$\begin{bmatrix} M_u & 0\\ 0 & -M_p\end{bmatrix}\begin{Bmatrix}\ddot{U}\\ \ddot{\psi}\end{Bmatrix}+\begin{bmatrix} 0 & C_{up}\\ C_{up}^T & 0\end{bmatrix}\begin{Bmatrix}\dot{U}\\ \dot{\psi}\end{Bmatrix}+\begin{bmatrix} K_u & 0\\ 0 & -K_p\end{bmatrix}\begin{Bmatrix}U\\ \psi\end{Bmatrix}=\begin{Bmatrix}F\\ 0\end{Bmatrix} \qquad (12)$$

THE PZT COUPLING MODELLING

A rectangular plate element has been taken into account to describe the PZT patch. Each node of the element have five mechanical dofs [9]. Since this element should represent a PZT lamina, an additional electrical dof is required, given by the charge q. We add the hypothesis that the electric plate is polarized in the transverse 3-direction. Moreover we assume a uniform charge density on upper and lower surfaces $D_3 = q/A$ (A being the surface normal to the direction of the electric field). The dofs vector may be expressed as follows:

$$x = \left\{u, v, w, \vartheta_x, \vartheta_y\right\}_{node} \cup q_{pzt} \qquad (13)$$

The reverse and direct effects of the piezoceramic device will be described in the following paragraphs, but let us introduce here the physical hypothesis by which the piezoceramic electromechanical matrices will be derived. Equations (14) represent the fluid structure coupled system in which the piezoceramic actuation and sensing capabilities, that is to say the reverse and direct effects have been modeled. The moment M_{pzt} and the voltage V_{pzt} will be derived according to the piezo constitutive equations. In other words, the actuation moment will be related to the electrical charge while the sensing voltage will be related to the mechanical dofs.

The fluid-piezo-structure matrix problem can then be written in the following form:

$$\begin{bmatrix} M_u & 0 & 0\\ 0 & -M_p & 0\\ 0 & 0 & 0\end{bmatrix}\begin{Bmatrix}\ddot{U}\\ \ddot{\psi}\\ \ddot{q}\end{Bmatrix}+\begin{bmatrix} 0 & C_{up} & 0\\ C_{up}^T & 0 & 0\\ 0 & 0 & 0\end{bmatrix}\begin{Bmatrix}\dot{U}\\ \dot{\psi}\\ \dot{q}\end{Bmatrix}+\begin{bmatrix} K_u & 0 & 0\\ 0 & -K_p & 0\\ 0 & 0 & C_{pzt}^{-1}\end{bmatrix}\begin{Bmatrix}U\\ \psi\\ q\end{Bmatrix}=\begin{Bmatrix}F+M_{pzt}\\ 0\\ V_{pzt}\end{Bmatrix} \qquad (14)$$

where C_{pzt} is the capacitor of the piezoelement.

In what follows, to simulate these effects only contact grid nodes between PZT and host structure will be taken into account.

PZT Reverse Coupling Matrix

In this paragraph the expression of the M_{pzt} has been derived according to the Crawley - De Luis strain actuation

model [5]. Let us recall the hypothesis of this theory for a piezo-structure sandwich:

- Linear stress/strain relation;
- Linear strain along the structure thickness;
- Constant strain along the piezo thickness;
- Stress/strain relation is negligible in the in-plane direction;
- Constant shear stress in the bonding layer.

In what follows the subscript *p*, *s* and *a* refers respectively to the piezo, the structure and the bonding layer. Expression have been reported and the reader is referred to the work of Lecce-Concilio [10]. In this paragraph let us just recall the main results but in [10] all the assumption on the mechanical boundary conditions can be found and the equilibrium equations for both the piezoceramic and the structure are the following ones:

$$\begin{aligned} \frac{d\sigma_p}{dx} - \frac{\tau}{t_p} &= 0 \\ \frac{d\sigma_s}{dx} + 6\frac{\tau}{t_s} &= 0 \end{aligned} \tag{15}$$

Substituting the stress expressions from the constitutive equations of the piezoceramic, the structure and the bonding layer, equation (15) can be rewritten as follows:

$$\begin{aligned} \frac{d^2\varepsilon_p}{dx^2} - \frac{G_a / E_p}{t_p}(\varepsilon_p - \varepsilon_s) &= 0 \\ \frac{d^2\varepsilon_t}{dx^2} + 6\frac{G_a / E_s}{t_a t_s}(\varepsilon_p - \varepsilon_s) &= 0 \end{aligned} \tag{16}$$

where G_a is the shear modulus of the bonding layer and E is the Young modulus referred to the pzt and the structure. By the integration of the (16) and introducing the following parameters:

$$\Psi = \frac{E_s t_s}{E_p t_p} \tag{17}$$

$$\Gamma^2 = \left(\frac{L}{2}\right)^2 \frac{G_a / E_p}{t_a t_p}\left(\frac{\Psi + 6}{\Psi}\right) \tag{18}$$

$$\Lambda = \frac{d_{31}}{t_p} V \tag{19}$$

representing the stiffness ratio, the bonding quality factor and the piezoceramic free strain at unitary voltage respectively, the expression of the strain actuation will be derived as follows:

$$\begin{aligned} \frac{\varepsilon_p}{\Lambda^2} &= \frac{6}{\Psi + 6} + \frac{\Psi}{\Psi + 6}\frac{\cosh \Gamma x}{\cosh \Gamma} \\ \frac{\varepsilon_s}{\Lambda^2} &= \frac{6}{\Psi + 6} - \frac{6}{\Psi + 6}\frac{\cosh \Gamma x}{\cosh \Gamma} \end{aligned} \tag{20}$$

Finally the piezoceramic moment, in case of perfect bonding, is:

$$M_{pzt} = D_{uq}\, q \tag{21}$$

with

$$D_{uq} = \frac{3}{2}\frac{1}{\Psi + 6} E_s t_s^2 L_p \frac{d_{31}}{C_{pzt}\, t_p}$$

The use of this relation between the actuator moment and electric charge allow us to express equation (14) in the following form:

$$\begin{bmatrix} M_u & 0 & 0 \\ 0 & -M_p & 0 \\ 0 & 0 & 0 \end{bmatrix} \begin{Bmatrix} \ddot{U} \\ \ddot{\psi} \\ \ddot{q} \end{Bmatrix} + \begin{bmatrix} 0 & C_{up} & 0 \\ C_{up}^T & 0 & 0 \\ 0 & 0 & 0 \end{bmatrix} \begin{Bmatrix} \dot{U} \\ \dot{\psi} \\ \dot{q} \end{Bmatrix} + \begin{bmatrix} K_u & 0 & -D_{uq} \\ 0 & -K_p & 0 \\ 0 & 0 & C_{pzt}^{-1} \end{bmatrix} \begin{Bmatrix} U \\ \psi \\ q \end{Bmatrix} = \begin{Bmatrix} F \\ 0 \\ V_{pzt} \end{Bmatrix} \tag{22}$$

At this point is necessary to build the finite element formulation in order to evaluate the D_{uq} matrix. For this we can split the value of the moment (21) in the number of the nodes along *x* and *y* directions, in which the pzt has been discretised. Figure 1 is an example of a piezoceramic actuation experienced on the contact grid nodes. The arrows show the contribution of the moment for each node.

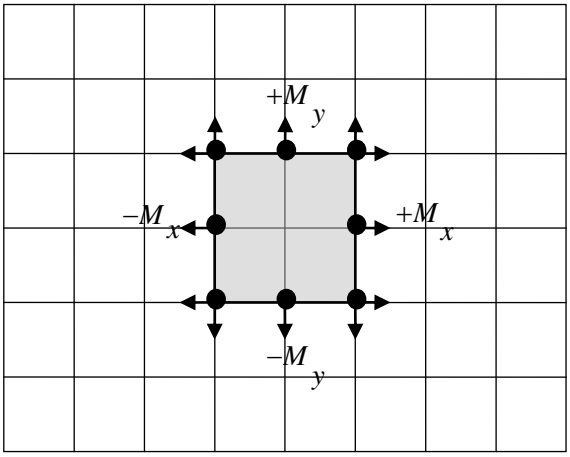

Figure 1. PZT actuation over the hosting structure

Now the matrix can be assembled, the dimension is $n \times 1$where n is the total number of mechanical dofs of the system. For simplicity (23) refers to the nodes, each node having 5 mechanical dofs.

$$D_{uq} = \begin{bmatrix} node1 \\ node2 \\ . \\ . \\ noden \end{bmatrix}_{n\times 1} \quad (23)$$

This vector has all zero elements except the ϑ_x and ϑ_y components of the grid nodes associated with the border of the piezoceramic element.

PZT Direct Coupling Matrix

In this paragraph the expression of the V_{pzt} has been derived. The PZT direct coupling matrix that links piezo deformation to the voltage may be estimated by computing the second derivative of the transversal displacement *w*, from the following assumptions:

- Bending-torsion coupling negligible;
- Axial vibrations negligible;
- Voltage not coupled to the axial vibrations;
- Electric field along the transversal direction;
- Constant charge in the surface;
- Isotropic material.

From the piezoceramic constitutive equations, according to the previous assumptions, we have:

$$D_z = \begin{bmatrix} d_{31} & d_{31} & 0 \end{bmatrix} \begin{Bmatrix} \sigma_{xx} \\ \sigma_{yy} \\ \tau_{xy} \end{Bmatrix} \quad (24)$$

where

$$\begin{Bmatrix} \sigma_{xx} \\ \sigma_{yy} \\ \tau_{xy} \end{Bmatrix} = \frac{E_p}{1-\nu^2} \begin{bmatrix} 1 & \nu & 0 \\ \nu & 1 & 0 \\ 0 & 0 & \frac{1-\nu}{2} \end{bmatrix} \begin{Bmatrix} \varepsilon_{xx} \\ \varepsilon_{yy} \\ \gamma_{xy} \end{Bmatrix}$$

The corresponding in plane stresses, according to the Kirchhoff plate model, can be related to the transversal displacement in the classical way:

$$\varepsilon_{xx} = -z\frac{\partial^2 w}{\partial x^2} \qquad \varepsilon_{yy} = -z\frac{\partial^2 w}{\partial y^2} \quad (25)$$

in which only flexural movement have been taken into account.

Finally, the voltage has been related to the mechanical dofs (through the (i,j) coordinates of the nodes of interest) by the following relation (see Figure 2):

$$V_{pzt} = g_{31}\frac{E_p t_p (t_p + t_s)}{2(1-\nu)}\left[\frac{w_{i-1,j} - 2w_{i,j} + w_{i+1,j}}{\Delta x^2} + \frac{w_{i,j-1} - 2w_{i,j} + w_{i,j+1}}{\Delta y^2}\right] \quad (26)$$

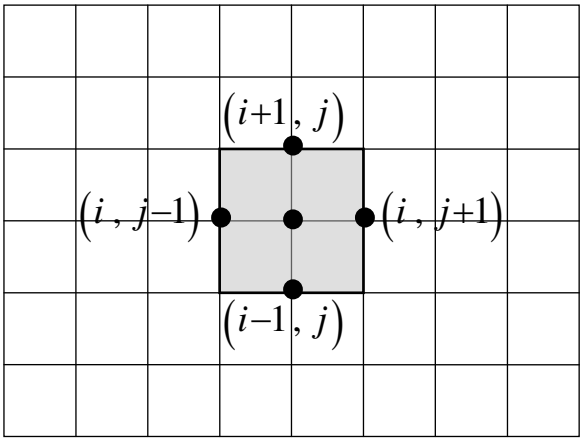

Figure 2. PZT sensing over the host structure

The matrix G_{qu} (such that $V_{pzt} = G_{qu}U$) must be also obtained by assembling the nodes contributions:

$$\left[G_{qu}\right]U = g_{31}\frac{E_p t_p (t_p + t_s)}{2(1-\nu)}\left(\frac{1}{\Delta x^2} + \frac{1}{\Delta y^2}\right)\sum_1^n \left[...w_l...\right]_{1\times n} \quad (27)$$

Equation (27) is a $1\times n$ row where *n* is the total number of the mechanical dofs. Each elements of this vector are null except those corresponding to the transversal displacement of the contact grid nodes indicated in Figure 2. The (22) can be written as:

$$\begin{bmatrix} M_u & 0 & 0 \\ 0 & -M_p & 0 \\ 0 & 0 & 0 \end{bmatrix} \begin{Bmatrix} \ddot{U} \\ \ddot{\psi} \\ \ddot{q} \end{Bmatrix} + \begin{bmatrix} 0 & C_{u\varphi} & 0 \\ C_{u\varphi}^T & 0 & 0 \\ 0 & 0 & 0 \end{bmatrix} \begin{Bmatrix} \dot{U} \\ \dot{\psi} \\ \dot{q} \end{Bmatrix} + \begin{bmatrix} K_u & 0 & -D_{uq} \\ 0 & -K_p & 0 \\ -G_{qu} & 0 & C_{pzt}^{-1} \end{bmatrix} \begin{Bmatrix} U \\ \psi \\ q \end{Bmatrix} = \begin{Bmatrix} F \\ 0 \\ 0 \end{Bmatrix} \quad (28)$$

THE CIRCUIT PARAMETERS

To finally describe the circuit, the *R* and *L* representing respectively the inductor and the resistor components, have been added to the model. The final expression of the dynamics equations for the coupled system is the following one:

$$\begin{bmatrix} M_u & 0 & 0 \\ 0 & -M_p & 0 \\ 0 & 0 & L \end{bmatrix} \begin{Bmatrix} \ddot{U} \\ \ddot{\psi} \\ \ddot{q} \end{Bmatrix} + \begin{bmatrix} 0 & C_{u\varphi} & 0 \\ C_{u\varphi}^T & 0 & 0 \\ 0 & 0 & R \end{bmatrix} \begin{Bmatrix} \dot{U} \\ \dot{\psi} \\ \dot{q} \end{Bmatrix} + \begin{bmatrix} K_u & 0 & -D_{uq} \\ 0 & -K_p & 0 \\ -G_{qu} & 0 & C_{pzt}^{-1} \end{bmatrix} \begin{Bmatrix} U \\ \psi \\ q \end{Bmatrix} = \begin{Bmatrix} F \\ 0 \\ 0 \end{Bmatrix} \quad (29)$$

The integration in time domain provides the response of the system with and without control for the mode of interest.
Let us briefly describe the behaviour of the switch control, in order to define the best values of the parameters. The

piezoelement, generally in open circuit state switches to short circuit state for a fraction of the considered excitation period. During the closed circuit state, the inductance allows a charge inversion on the PZT electrodes (see Figure 3).

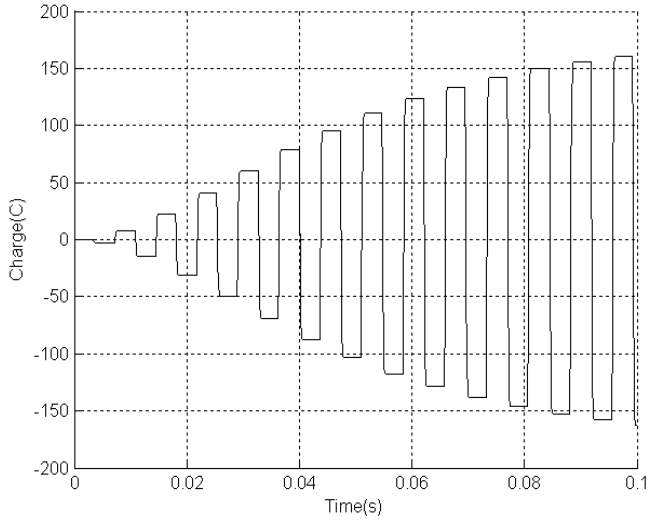

Figure 3. PZT charge during the switch control for the first resonance frequency

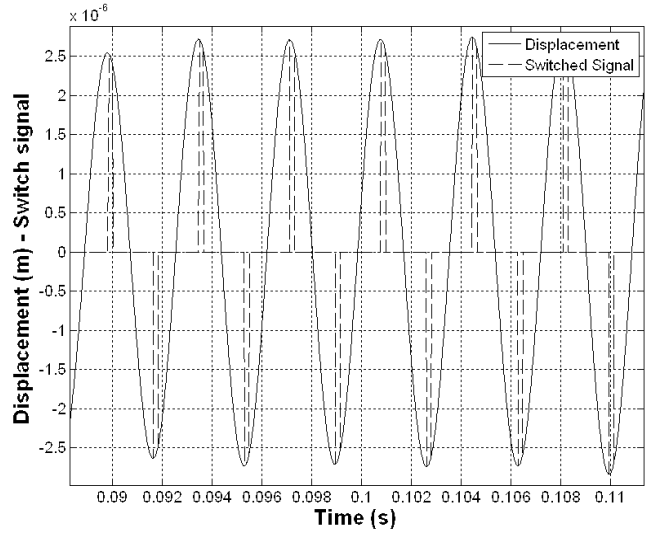

Figure 4. Time evolution of the switch signal

In other words, when the charge is inverted, the piezo can perform a local strain actuation in phase opposition with respect to the structural strain. This phenomenon generates damping through a "pulse train" signal, in Figure 4 the switch signal synchronized with the maxima strain.

The electrical oscillation should be designed to be "independent" on the structure dynamics, that is to say it must be "enough" high if compared with the highest mechanical resonance frequency to be controlled. Previous results [4-9] show a good behavior for a switching period of 1/10 of the highest resonance frequency to be controlled.
The circuit pulsation ω_{el} is simply related to C_{pzt} and L through the well known relation:

$$\omega_{el} = 10\omega_{mech} = \frac{1}{\sqrt{C_{pzt}L}} \tag{30}$$

Moreover, since the working principle of the SSC system is characterized by fast state variations, due to the electric circuit quick commutation times, the system behaviour will suffer a continuous transient regime. In what follows a computation in the time domain will be performed using a direct implicit numerical scheme of the Newmark family algorithm will be used.

The transient structural output is computed using a couple of equations, assuming the short circuit/open circuit state. The integration method may be schematized as follows (Figure 5).

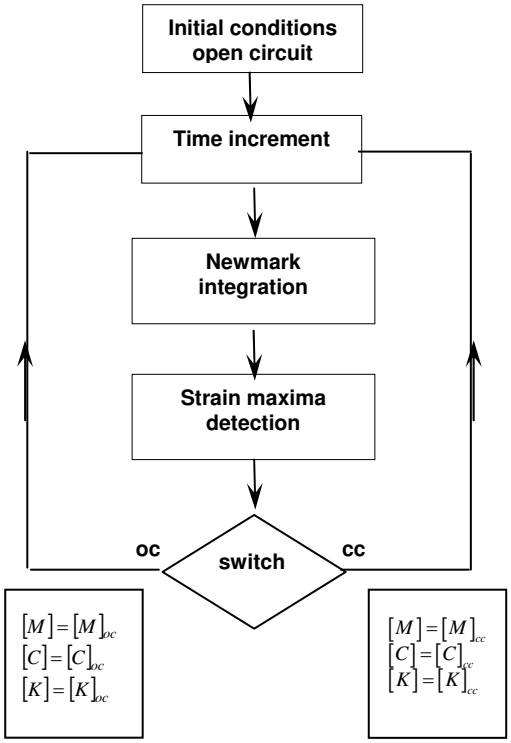

Figure 5. SSC-Newmark integration method flow chart

As illustrated in the previous flowchart, after the time integration performed by a Newmark algorithm, the maxima are detected through a standard sine signal inversion procedure. When a maximum of strain is reached, the circuit is closed (Closed-Circuit configuration). The circuit remains in this state for the designed time interval. If no maxima are detected, the system is switched to an Open-Circuit configuration. In the

following Table 1, are summarized the electrical parameter adopted in the numerical simulation of the control:

State	OC	CC
Electrical frequency	-	10 × Mech Freq
R (Ohm)	10^{10}	100
L (Henry)	-	see equation (30)
C_{pzt} (Farad)	221×10^{-9}	221×10^{-9}

Table 1. Open and short circuit parameters

TEST CAMPAIGN: DESCRIPTION AND RESULTS

Referring to the experimental test [3], the system consists of the same rigid cavity filled with air with, with an aluminium plate with all clamped edges at one end, and a PZT patch bonded in the centre. Let us notify that in our model the thickness of the plate and that of the PZT are of 1 mm and 0.5 mm, respectively. Moreover, let us recall that we are dealing with a semi-active control system with no damping layer added to the model, differently by [3]. In the following figure (Figure 6) is sketched the acoustic cavity:

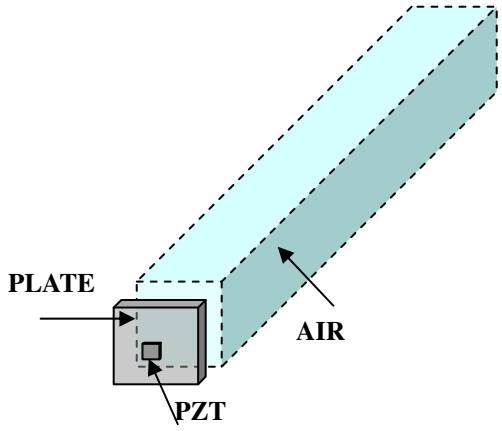

Figure 6. Acoustic cavity to be modelled with finite elements

Table 2, 3 and 4 define the geometrical and mechanical characteristics of the test specimen:

PLATE	
Material	Alluninum 7075-T6
In-plane dimensions (m)	0.30×0.30
Thickness (m)	0.001
Young modulus (GPa)	72
Poisson ratio	0.33
Density (kg/m^3)	2700

Table 2. Plate mechanical and geometrical parameters

FLUID BOX	
Material	Air
Dimensions (m)	0.30×0.30×0.75
Sound velocity (m/s)	340
Density (kg/m^3)	1225

Table 3. Fluid geometrical and physical parameters

PZT	
Material	PPK-11 Stettner
In-plane dimensions (m)	0.05×0.05
Thickness (m)	0.0005
Young modulus (GPa)	59
Poisson ratio	0.34
Density (kg/m^3)	2700
g_{31} (Vm/N)	8.0e-3
d_{31} (C/N)	3.5e-10

Table 4. PZT mechanical and geometrical parameters

Modal analysis

In order to validate the finite element implementation of the proposed model, in what follows are presented the computation of the eigenvalues of the plate, the cavity and the coupling system respectively, according to the main finite element characteristics in the following tables (see Tables 5, 6):

PLATE FEM	
Finite Element	QUAD4
Mesh discretization	10×10
N° nodes	121
N° constrained nodes	40
Total number of dofs	486
Constrained type	Four clamped edges

Table 5. Plate finite element model parameters

Mode_1 **Mode_2**

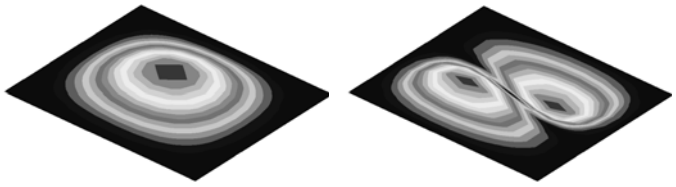

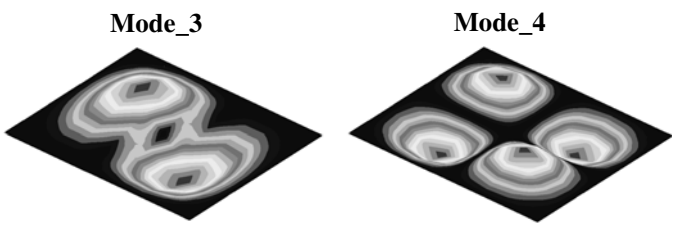

Figure 7. First four modal shapes of the clamped plate

FLUID BOX FEM	
Finite element	HEXA8
Mesh discretization	10×10×25
Total number of dofs	3146

Table 6. Fluid finite element model parameters

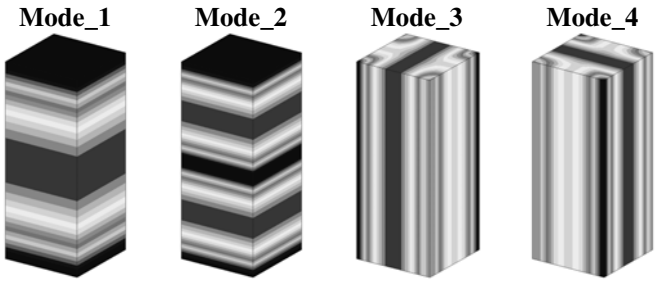

Figure 8. First four air cavity modal shapes

PLATE Freq (Hz)		FLUID Freq (Hz)		F-S Freq (Hz)
Nastran	**Exact**	**Nastran**	**Exact**	**Nastran**
99	95	213	219	96
201	197	432	438	200
201	197	569	576	200
290	285	569	576	217

Table 7. Eigenfrequencies

The previous Table 7 presents the first four eigenfrequencies for the system. The exact solutions are referred to Blevins [13]. Of course more accordance can be achieved through a refined mesh discretization. In Figure 9 is sketched the model with the external excitation and the location at witch the vibrations and sound pressure level will be detected.

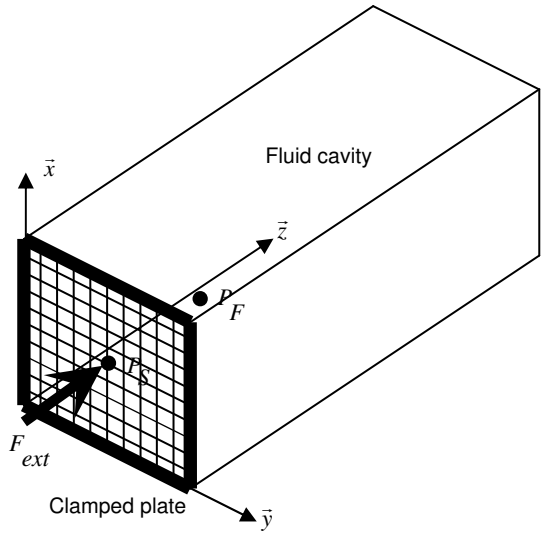

Figure 9. Acoustic cavity: FEM and boundary conditions

SSC results in time domain

The plate is excited with a pure sinusoidal wave at the first resonance frequency. The vibration output is detected in the centre of the plate where the displacement reaches a maximum; the pressure level is detected inside the cavity along the axial line of the cavity at 15 cm from the plate. The structural and pressure level are plotted in time domain. Moreover, the damping capability of the SSC is evaluated by:

$$d = 20\log_{10}\frac{A_{co}}{A_{nc}}$$

where A is the amplitude of the signal and the subscript *co* and *nc* refers to the controlled and non controlled system status.

In the Figures 10 to 14 the results for the first mode have been plotted. Previous results [4] performed on the structural damping through the SSC technique shows wide band control efficiency. In the present work, since the goal has been to study the feasibility of the semi passive control on the noise reduction, just the first mode has been processed.

A first test is carried out without structural damping showing just the effect of the perturbation introduced by the circuit. In Figure 10, two plots have been presented, the first on the structural displacement and the second on the interior pressure level.

In the second step, a proportional damping is added to the system being the structural damping coefficient ξ as 0.01. Again results have been reported in time domain with the relative spectrum signal for both the structural displacement and pressure level (Figures 11 and 12). Finally, taking into account the experimental test of [8], voltage amplification is introduced, in order to enhance the damping performances of the synchronized switch control technique (Figures 13 and 14).

Mode 1: no structural damping

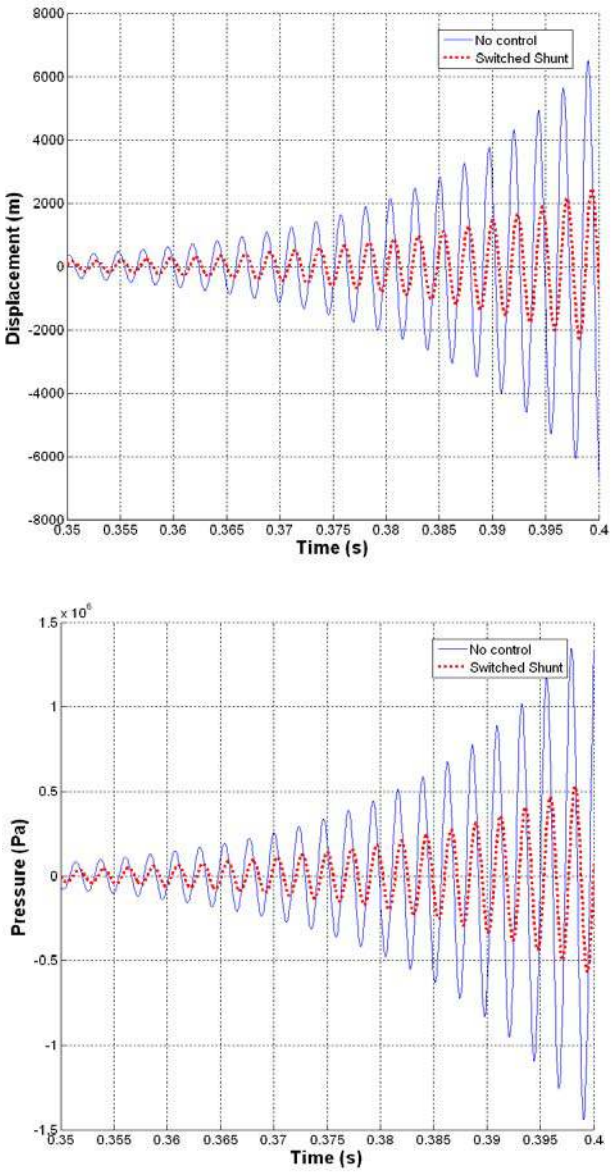

Figure 10. Time evolution for the first frequency. Up: structural vibration; Down: pressure level

The results plotted in Figure 10 refers to the time evolution of the displacement of the plate detected in the central node and to the sound pressure level detected at a distance of 15 cm from the plate surface in the inward direction. The straight line is the evolution of the system without control while the dotted line is the evolution with the synchronized switch control. Since no damping has been added to the system a typical diverging behavior can be observed. Anyway the effect of the control on both the structure and the fluid has been achieved.

Mode 1: structural damping with ξ=0.01

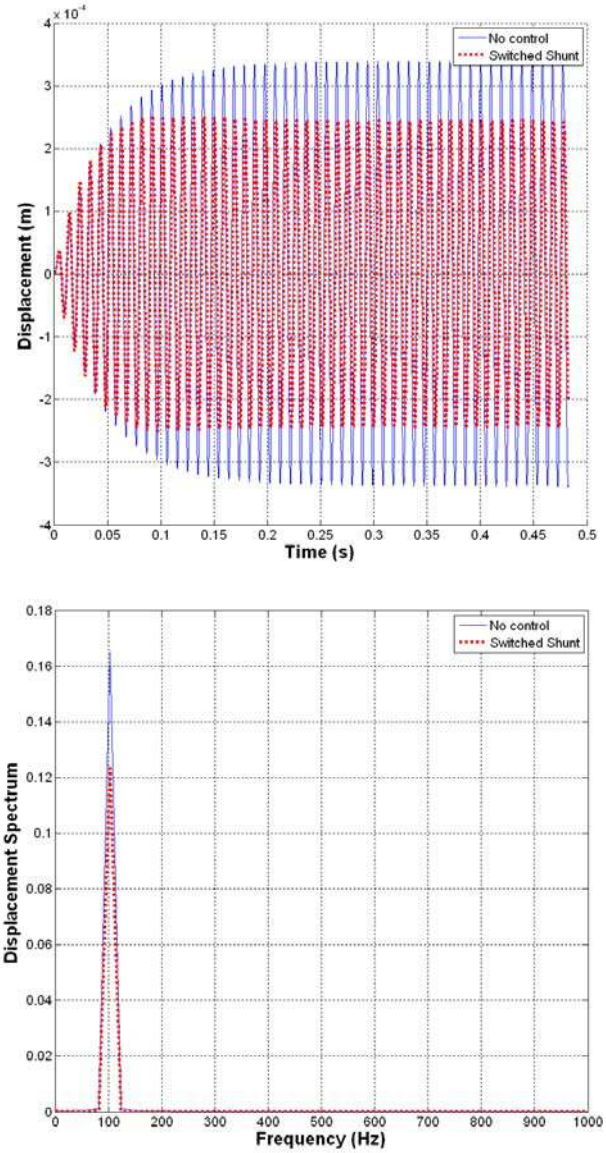

Figure 11. First frequency. Up: time evolution of structural vibration; Down: spectrum of displacement

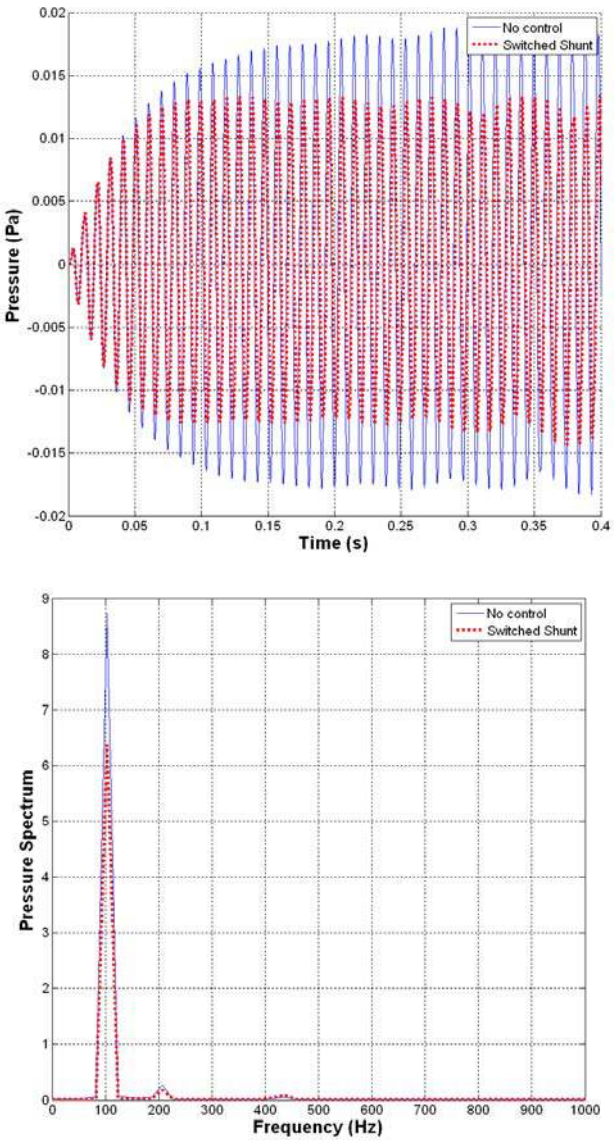

Figure 12. The first frequency. Up: time evolution of pressure level; Down: spectrum of pressure

The results plotted in Figure 11 refers to the time evolution of the displacement of the plate detected in the central node and the results of Figure 12 refers to the sound pressure level detected at a distance of 15 cm from the plate surface in the inward direction. The straight line is the evolution of the system without control while the dotted line is the evolution with the synchronized switch control. In this test a proportional damping is added to the system, being the structural damping coefficient 0.01. The effect of the control on both structure and fluid has been achieved, and after the typical transient period, a regime condition can be observed. Some beatings can also be observed in the sound pressure level evolution. This phenomenon can be easily justified observing the pressure spectrum plot. It is possible to note the second pick at 210 Hz and the third pick at 430 Hz that shows the structural excitation along the z direction, has been able to excite the first two fluid modes.

Mode 1: structural damping with ξ=0.01 and voltage amplification

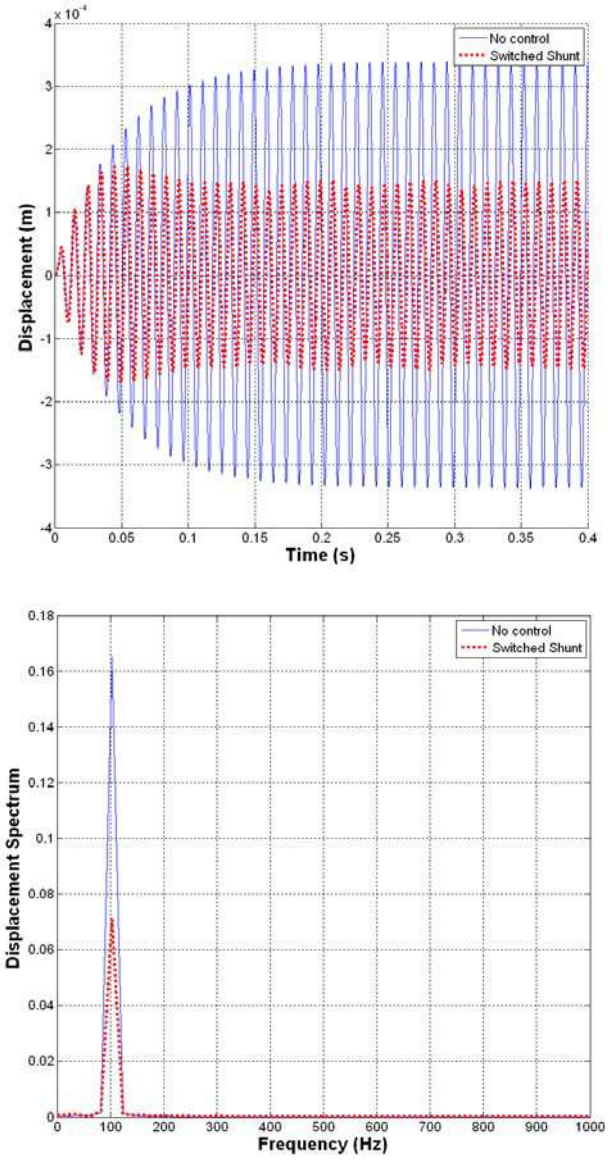

Figure 13. The first frequency. Up: time evolution of structural vibration; Down: spectrum of displacement.

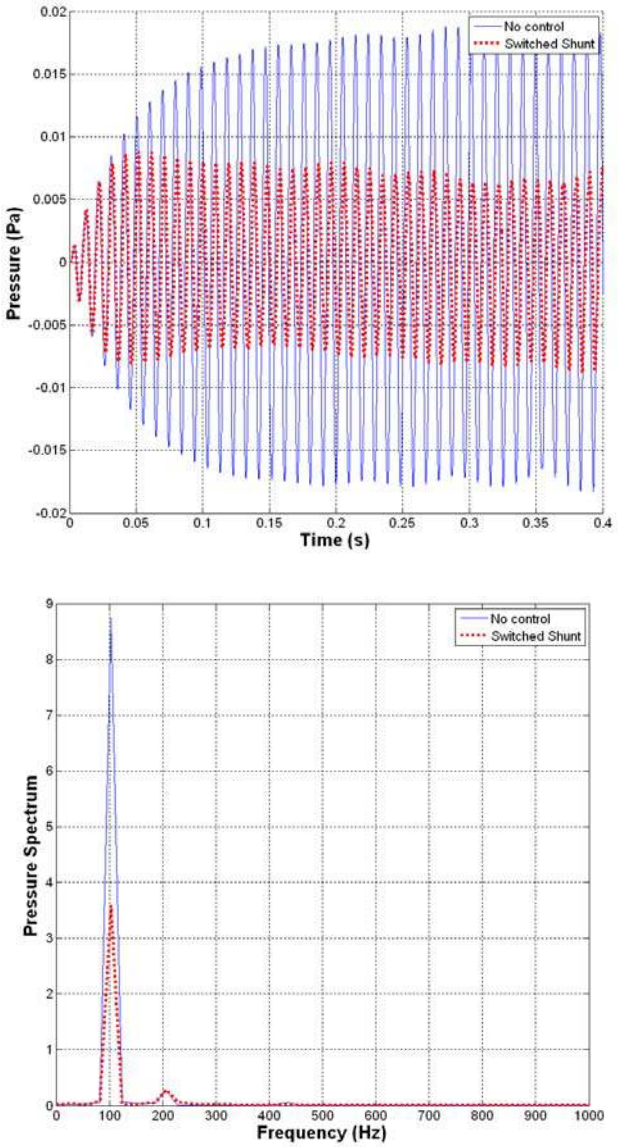

Figure 14. The first frequency. Up: time evolution of pressure level; Down: spectrum of pressure

The results plotted in Figure 13 refers to the time evolution of the displacement of the plate detected in the central node and the results of Figure 14 refers to the sound pressure level detected at a distance of 15 cm from the plate surface in the inward direction. The straight line is the evolution of the system without control while the dotted line is the evolution with the synchronized switch control. In this test the same proportional damping of the previous test has been left to the system, but now some voltage amplification is introduced.

In the table below (Table 8) the damping effect is expressed in dB for the first resonance frequency at different voltage driving source.

Mode	1st	1st
Gain Voltage	1	2
Vibration (dB): node 81	3.31	9.24
SPL (dB): node 1119	3.15	9.04

Table 8. The vibration and pressure level reduction in dB at different voltage driving source

CONCLUSIONS

In this paper we have presented numerical results concerning vibration reduction of structural-acoustic systems using the synchronized switch control technique. The experiments showed that reduction of vibrations can be achieved for the first resonance frequency using piezoelectric patch on the centre of the plate, connected to the *RL* electrical components. No optimization process has been done to determine the best position for the actuators to a multimodal control purpose. In this work just the first modal shape can be optimally controlled, according to the maximum strain of the plate (let us recall that for the particular geometry and boundary conditions the maximum is reached in the center of the plate). The results show also that some beatings are present due to the excitation of the first and second resonance frequency of the fluid. Some amplification has been added to drive the PZT actuator in order to augment the effectiveness of the control, taking into account the results presented in [8].
In order to improve the damping capability of the semi passive control system here adopted, the further improvement steps should be taken into account:

- piezoelectric location on the structure is a fundamental point that has to be considered in order to improve the damping;
- the switch mechanism introduces a high frequency noise that can be reduced using viscoelastic treatments.

ACKNOWLEDGMENTS

This study is part of the PhD sponsored by the European Community through the Marie Curie Research Training Network "A Computer Aided Engineering Approach to Smart Structures Design" under contract number MRTN-CT-2006-035559.

REFERENCES

[1] Morand, H.J.-P., Ohayon, R., Fluid structure interaction, Wiley, 1995.
[2] Deü, J.-F., Larbi, W. and Ohayon, R., "Piezoelectric structural acoustic problems: Symmetric variational formulations and finite element results", *Computer*

Methods in Applied Mechanics and Engineering, **197** (19-20), pp. 1715-1724, 2008.

[3] Ro, J. and Baz, A., "Control of sound radiation from a plate into an acoustic cavity using active constrained layer damping", *Smart Material and Structures*, **8**, pp. 292-300, 1999.

[4] Ciminello, M., Ameduri, S., Concilio, A., Lecce, L., "Flow-chart design of a PZT network based on a Switched Shunt Control", *Actuator 2008, 11th International Conference on New Actuators*, Bremen, Germany, 9-11, pp. 957-960, 2008.

[5] Crawley, E.F. and J. de Luis, "Use of piezoelectric actuators as elements of intelligent structures", *AIAA Journal*, **25** (10), pp. 1373-1385, 1998.

[6] Kim, J. and Ko, B., "Optimal design of a piezoelectric smart structure for noise control", *Smart Material and Structures*, **7**, pp. 801-808, 1998.

[7] Ro, J. and Baz, A., "Control of sound radiation from a plate into an acoustic cavity using active constrained layer damping", *Smart Material and Structures*, **8**, pp. 292-300, 1999.

[8] Guyomar, D., Richard, T. and Richard, C., "Sound wave transmission reduction through a plate using a piezoelectric synchronized switch damping technique", *Journal of Intelligent Material Systems and Structures*, published online, 2008.

[9] Ciminello, M., Ameduri, S., Concilio, A., "FE Modelling of an Innovative Vibration Control Shunt Technique", *Journal of Intelligent Materials Systems and Structures*, published on line, 2007.

[10] Concilio A., "Controllo attivo del rumore in cabina mediante attuatori piezoelettrici distribuiti sulla struttura", PhD Thesis in Aerospace Engineering, University of Naples "Federico II", 1992, www.dpa.unina.it

[11] J. S. Han, E. B. Rudnyi, and J. G. Korvink, "Efficient optimization of transient dynamic problems in mems devices using model order reduction", *Journal of Micromech. Microeng*., **15**, pp. 822–832, 2005.

[12] E. B. Rudnyi, J. Lienemann, A. Greiner, and J. G. Korvink, Generating Compact Models Directly from ANSYS Models, in *Proc.NSTI-Nanotech*, (2), Boston, USA, pp. 279–282, 2004.

[13] Blevins R.D., "Formulas for natural frequency and mode shape", Krieger Publishing Company, Malabar Florida, 1993.